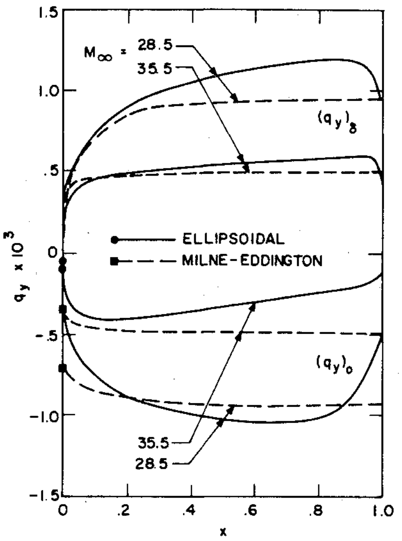

Fig. 3 Flux distributions to wedge surface and stream, in surface normal direction, $\theta_w = 0.61$ rad, $(M_\infty, \tau_L, Bo) = (28.5,\ 0.62,\ 0.027)$ and $(35.5,\ 5.42,\ 0.0092)$.

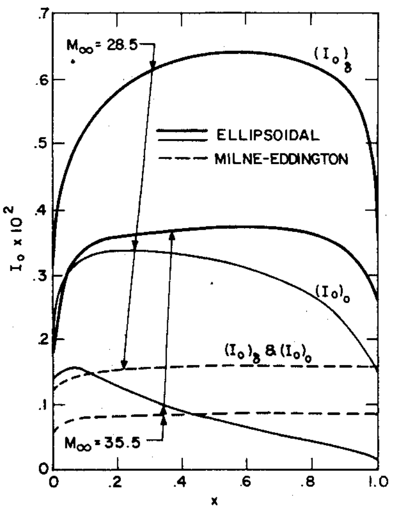

Fig. 4 Intensity distributions along surface and shock, $\theta_w = 0.61$ rad, $(M_\infty \tau_L, B_0) = (28.5,\ 0.62,\ 0.027)$ and $(35.5, 5.42, 0.0092)$.

$\alpha_s = 0.355$/m, and $\sigma T_s^4 = 9 \times 10^9$ W/m^2. Boltzmann and Bouguer numbers are defined as $Bo = (\rho uh/\sigma T^4)_s$ and $\tau_L = \alpha_s L$, with $L = 1.75$ m for an assumed 1-m base height. All numerical values correspond to Ref. 1 to enable comparison. For these conditions, emission is appreciably larger than absorption and the significant differences in I_0 for *M.E.* and ellipsoidal modeling imply negligible differences in the corresponding strongly coupled fluid field.

The surface parallel flux q_{x_0} is indicative of the modeling importance (Fig. 2). This is consistent with the pure radiation field studies[4,5] that pointed out the errors in *M.E.* for flux components not constrained by the boundary condition. *M.E.* failure is clear, in fact, from the $|q_x| \approx 7I_0$ result (see Fig. 4) at the nose, whereas moment definitions require $|q_x| \leq I_0$. The comparison is not as poor at the downstream boundary where the matching of average (for the integral method) I_0 and q_x are imposed.

The normal flux component, q_{y_0}, provides surface heating (Fig. 3). Increasing M_∞ (or wedge angle[5]) leads to stronger shocks and the increasingly dominant radiation over convection (i.e., decreasing *Bo*) implies significant radiative cooling over a lesser distance. This effect tends to offset the increased absorption at the nose and results in a moderate increase in the actual (longitudinal) optical depth ($\int \alpha dx$) despite a considerable increase in the nominal $\alpha_s L$. Near the base, the transverse optical depth actually decreases. The influence of earlier cooling is absent from *M.E.* The overprediction of *M.E.* nose heating by a factor of six is especially important, and is associated with the boundary condition $q_{y_0} = -I_0/\sqrt{3}$, even in situations where the intensity concentration is in the xz plane. The areas between the q_{y_0} and q_{y_δ} distributions in Fig. 3 are a measure of the total fluid energy loss, and the reasonable agreement between *M.E.* and ellipsoidal methods is a consequence of the emission dominance.

Differences in I_0 fields (Fig. 4) between the methods indicate the appreciably different flowfields that must be expected with increasing absorption. The essentially constant I_0 distributions for *M.E.* are even more striking than the disagreement in magnitude. This behavior may be traced to the *M.E.* flux constraint $\mathrm{d}I_0/\mathrm{d}y \sim q_y$ which, for geometrically thin layers, implies large q_y for any significant I_0 change. However, for emission dominance, the integrated q_y must be accurate, limiting I_0 variations normal to the surface. The implications extend beyond a poor absorption representation to imposing virtually identical outward fluxes at both surface and shock, since the *M.E.* normal flux is related there to the local I_0. This is apparent in the *M.E.* curves in Fig. 3, where half of the radiated energy issues from each lateral boundary.

Although reabsorption may be relatively small everywhere ($M_\infty = 28.5$), in some situations ($M_\infty = 35.5$) reabsorption and emissions are comparable near the base (for either *M.E.* or ellipsoidal). Physically, this tends to diminish the surface-directed radiation by reabsorption and subsequent isotropic re-emission. The net effect is that more than half of the energy is radiated out through the shock, as made clear by the ellipsoidal results in Fig. 3. Thus, even in instances of overall insignificant reabsorption, the modeling is of some importance to the distributed absorption influence.

References

[1] Gibeling, H. J. and Baron, J. R., "Minimum Radiative Transfer Geometries," *Journal of Computers and Fluids*, Vol. 1, Jan. 1973, pp. 379-398.

[2] Jischke, M., "Radiation Coupled Wedge Flows," *AIAA Journal*, Vol. 4, July 1966, pp. 1300-1302.

[3] Olfe, D. B., "Radiative Cooling in Transparent Shock Layers of Wedges and Cones," *AIAA Journal*, Vol. 4, Oct. 1966, pp. 1734-1740.

[4] Elgin, J. B. and Baron, J. R., "A Variable Closure Differential Approximation for Anisotropic Radiation," *Journal of Quantitative Spectroscopy and Radiative Transfer*, Vol. 16, Oct. 1976, pp. 805-818.

[5] Elgin, J. B., "Anisotropic Radiative Transfer in Gas Dynamics," Ph.D. Thesis, Feb. 1976, Massachusetts Institute of Technology, Cambridge, Mass.; also, TR-75-1564, Air Force Office of Scientific Research, 1975.

[6] Vincenti, W. G. and Kruger, C. H., *Introduction to Physical Gas Dynamics*, Wiley, New York, 1965, Chap. 12.

[7] Zeldovich, Y. B. and Raizer, Y. D., *Physics of Shock Waves and High Temperature Hydrodynamic Phenomena*, Vol. 1, Academic Press, New York, 1967, Chap. 2.

Radiative Ablation of Melting Solids

Anant Prasad* and S.N. Sinha†

Regional Institute of Technology, Jamshedpur, India

Nomenclature

c	= heat capacity per unit volume of the solid
H	= heat flow vector
k	= thermal conductivity of the solid
L	= latent heat of the solid
$q_1(t)$	= unknown surface temperature
$q_2(t)$	= melting distance
t	= time

Received April 28, 1976; revision received July 6, 1976.

Index categories: Heat Conduction; Material Ablation.

*Assistant Professor, Department of Mechanical Engineering.

†Lecturer, Department of Metallurgical Engineering.

T_f = temperature of the surroundings
α = thermal diffusivity
β = dimensionless temperature of the surroundings, $cT_f/\rho L$
η = dimensionless melting distance, $\epsilon\sigma T_f^3 q_2/k$
ϵ = emissivity of the solid
σ = Stephan-Boltzmann constant
θ = temperature distribution in the melt
ρ = density of the solid
τ = dimensionless time, $\epsilon^2\sigma^2 T_f^7 t/\rho Lk$
ϕ = dimensionless surface temperature, q_1/T_f

Introduction

RADIATIVE ablation occurs in melting solids when a large temperature difference exists between the solid and the surroundings from which the solid receives heat. This is actually a phase change problem and its exact solution has not been obtained, although a number of approximate methods are available that can be used with ease to analyze such a problem. In the past, one of the approximate methods called Biot's variational method was applied to solve a number of such phase-change problems,[1-3] and more recently the first of the present authors[4-6] solved problems of this kind where ablation of melting solids was considered due to aerodynamic and constant heat flux heating. In the present paper, closed-form solutions are obtained for melting distance and the surface temperature when the ablation occurs in the melting solid as a result of radiative heating. A numerical solution also is obtained.

Formulation of the Problem

The melting solid is considered in the form of a semi-infinite solid to which one-dimensional radiative heating is applied. The solid has a constant cross-sectional area, and its thermophysical properties are constant and the same, both in the solid and the molten regions. After initiation of the melting, T_f and $q_1(0,t)$ are assumed to be the temperature of the surroundings and the surface of the melt, respectively, whereas $q_2(t)$ is the distance of the melt line from the surface after time t. This time t is measured from the initiation of melting. Although a temperature distribution exists in the solid, it is simplified by assuming the whole solid at melting temperature. The validity of this assumption was demonstrated earlier.[7] The equation which governs this problem is

$$\partial^2\theta/\partial x^2 = (1/\alpha)\partial\theta/\partial t \qquad x>0,\ t>0 \tag{1}$$

Initial and boundary conditions are

$$\theta = 0 \qquad t=0 \tag{2}$$

$$q_2(t)=0 \qquad t=0 \tag{3}$$

$$-k\partial\theta/\partial x = \epsilon\sigma(T_f^4 - q_1^4) \qquad x=0,\ t>0,\ T_f>q_1 \tag{4}$$

Since the temperature assumed in the solid is uniform, an energy balance at the interface of the melt line gives the boundary condition

$$\dot{H} = \rho L\dot{q}_2 \qquad x=q_2(t), t>0 \tag{5}$$

where $\dot{H}$ represents the rate of heat flow with $H=\rho Lq_2$. The melting temperature is taken to be zero.

Solution

A linear temperature is assumed in the melt as

$$\theta = q_1(1-x/q_2) \tag{6}$$

where q_1 and q_2 are unknown generalized coordinates that are to be determined. They represent, respectively, the instant surface temperature and the instant melting distance. The conservation of energy equation is

$$\mathrm{Div}H = -c\theta \tag{7}$$

Using Eqs. (6) and (7) the heat flow field becomes

$$H=(½)cq_1q_2(1-x/q_2)^2+\rho Lq_2 \tag{8}$$

This equation satisfies the boundary condition (Eq. 5). Differentiating Eq. (8) with respect to time, the rate of heat flow becomes

$$\dot{H}=(½)c(q_1\dot{q}_2+\dot{q}_1q_2)(1-x/q_2)^2 + cq_1\dot{q}_2(x/q_2)(1-x/q_2)+\rho L\dot{q}_2 \tag{9}$$

By knowing the temperature distribution (Eq. 6), and heat flow field (Eq. 8), Biot's variational principle can easily be applied, which leads to the Lagrangian equation

$$\partial V/\partial q_2 + \partial D/\partial \dot{q}_2 = Q_2 \tag{10}$$

The functions V, D, and Q_2 correspond, respectively, to the thermal potential, thermal dissipation and thermal force and are

$$V=(½)\int_0^{q_2} c\theta^2 dx \tag{11}$$

$$D=(½k)\int_0^{q_2} \dot{H}^2 dx \tag{12}$$

$$Q_2=(\theta)_{x=0}(\partial H/\partial q_2)_{x=0} \tag{13}$$

Equation (6) together with Eq. (11) yields

$$V=(1/6)cq_1^2q_2 \tag{14}$$

$$\partial V/\partial q_2 = (1/6)cq_1^2 \tag{15}$$

Using Eqs. (9) and (12) we have

$$D=(½k)[(c^2q_2/20)(\dot{q}_1q_2+q_1\dot{q}_2)^2+(c^2q_1^2q_2\dot{q}_2^2/30) + \rho^2L^2q_2\dot{q}_2^2 + (\dot{q}_1q_2+q_1\dot{q}_2)(c^2q_1q_2\dot{q}_2/20 + c\rho Lq_2\dot{q}_2/3)+c\rho Lq_1q_2\dot{q}_2^2/3] \tag{16}$$

$$\partial D/\partial\dot{q}_2 = (q_2\dot{q}_2/2k)(2\rho^2L^2+4c\rho Lq_1/3+4c^2q_1^2/15) + (q_2^2\dot{q}_1/2k)(3c^2q_1/20+c\rho L/3) \tag{17}$$

Using Eq. (8), the partial differential of H with respect to q_2 becomes

$$\partial H/\partial q_2 = (½)cq_1(1-x/q_2)^2 + cq_1(x/q_2)(1-x/q_2)+\rho L \tag{18}$$

Substituting Eqs. (18) and (6) in Eq. (13), we have

$$Q_2=(½)cq_1^2+\rho Lq_1 \tag{19}$$

In generalized coordinate q_2, the Lagrangian equation (10) becomes

$$(q_2\dot{q}_2/30k)(30\rho^2L^2+20c\rho Lq_1+4c^2q_1^2)+(q_2^2\dot{q}_1/40k)(3c^2q_1+60c\rho L)=(⅓)(cq_1^2+3\rho Lq_1) \tag{20}$$

Using Eq. (6), the boundary condition in Eq. (4) becomes

$$k(q_1/q_2)=\epsilon\sigma(T_f^4-q_1^4) \tag{21}$$

Equation (21) introduces an additional relation between the generalized coordinates and reduces by one the number of differential equations of the Lagrangian type. Using nondimensional quantities (see nomenclature), Eqs. (20) and (21) become, respectively

$$\eta\dot{\eta}(120+80\beta\phi+16\beta^2\phi^2)+\eta^2\dot{\phi}(9\phi\beta^2+20\beta)=40\phi+40\phi^2\beta \tag{22}$$

$$\eta=\phi/(1-\phi^4) \tag{23}$$

Substituting Eq. (23) in Eq. (22) we have

$$\begin{aligned}&\dot{\phi}(B_1\phi+B_2\phi^2+B_3\phi^3/(1-\phi^4)^2\\&\quad+(B_4\phi^4+B_5\phi^5+B_6\phi^6)/(1-\phi^4)^3=A\phi+B\phi^2\end{aligned} \tag{24}$$

where

$$B_1=120 \qquad B_2=81\beta \qquad B_3=16\beta+9\beta^2 \qquad B_4=480$$

$$B_5=320\beta \qquad B_6=64\beta^2 \qquad A=40 \qquad B=40\beta$$

The solution of Eq. (24) gives the variation of surface temperature with time as

$$\begin{aligned}\tau=&\,[(B_4+B_5\phi+B_6\phi^2)/8(A+B\phi)(1-\phi^4)^2-B_4/8A]\\&+L_1\ln(1+B\phi/A)+(BL_2+L_8)\phi-L_3B\phi/(A+B\phi)\\&+L_4\tan^{-1}\phi+L_5\ln(1+\phi^2)-L_6\phi^2/(1+\phi^2)\\&+L_7\phi/(1+\phi^2)+L_9\phi^2+L_{10}\tanh^{-1}\phi+L_{11}\ln(1-\phi^2)\\&+L_{12}\phi^2/(1-\phi^2)+L_{13}\phi/(1-\phi^2)\end{aligned} \tag{25}$$

where

$$\begin{aligned}L_1=&\,(2B^4-A^4)/2B(B^4-A^4)[(B^2B_1^*-ABB_2^*-2AB_3)]+(1/4)[(-8A^3B/(B^4-A^4)^2\\&+4A^2(A^2+B^2)/V_1B+4A(B^2-A^2)/V_2](B^3B_4^*-ABB_5^*-2AB_6^*)+(1/4)(BB_5^*-2AB_6^*)\\&\cdot[2B/(B^4-A^4)+B(B^4-A^4)/V_1-B(B^2-A^2)^2/V_2]\end{aligned}$$

$$\begin{aligned}L_2=&\,(2B^4-A^4)(BB_2^*+B_3)/2B(B^4-A^4)^2+(1/4)[(-8A^3B/(B^4-A^4)^2+4A^2(A^2+B^2)/V_1B\\&+4A(B^2-A^2)/V_2](BB_5^*+B_6^*)+(B_6^*/4)(2B/(B^4-A^4)+B(B^4-A^4)/V_1-B(B^2-A^2)^2/V_1)\end{aligned}$$

$$\begin{aligned}L_3=&-A^2B_3(2B^4-A^4)/4B(B^4-A^4)^2-(A^2B_6^*/4)[(-8A^3B/(B^4-A^4)^2+4A^2(A^2+B^2)/V_1B\\&+4A(B^2-A^2)/V_2]+(1/4)[2B/(B^4-A^4)+B(B^4-A^4)/V_1-B(B^2-A^2)^2/V_2]\cdot(-B^2B_4^*+ABB_5^*-A^2B_6^*)\end{aligned}$$

$$\begin{aligned}L_4=&\,[(5B^2+3A^2)(AB_1^*-BB_2^*)-2B_3(2B^2+A^2)+4ABB_5^*-4(B^2-A^2)(B_4^*-B_6^*)]/8(A^2+B^2)^2\\&+[(4A^2B^2+B^2(B^2-A^2)^2)(B_4^*-B_6^*)-(4A^2B^3(A^2+B^2)-AB(A^2+B^2)^2-0.5(B^2-A^2)(A^2+B^2)]\cdot(1/4V_1)\end{aligned}$$

$$\begin{aligned}L_5=&\,[(A^2+2B^2)(AB_2^*-BB_1^*)-BB_3(1-A^2-B^2)-2ABB_4^*-B_5^*(B^2-A^2)]/8(A^2+B^2)^2\\&+[-4A^2B^3B_4^*(A^2+B^2)+B^2B_5^*(4A^2+(B^2-A^2)^2)-B_6^*(A^2+B^2)(2AB(A^2+B^2)+4A^2B^3)]/8V_1\end{aligned}$$

$$L_6=(B(B_1^*+B_3)-AB_2^*)/8(A^2+B^2)+(2AB(A^2+B^2)(B_4^*+B_6^*)+4A^2B^3B_5^*(A^2+B^2))/8V_1$$

$$L_7=(AB_1^*+BB_2^*)/8(A^2+B^2)+(A^2+B^2)^2(2ABB_5^*-B_4^*(B^2-A^2))/8V_1$$

$$\begin{aligned}L_8=&-(2ABB_5^*+B_6^*(B^2-A^2))/4(A^2+B^2)^2+(-4A^2B^3B_5^*(A^2+B^2)+B^2B_6^*(4A^2+(B^2-A^2)^2))/4V_1\\&+(BB_2^*-AB_3)/4(B^2-A^2)+(B^3B_2^*-AB^2B_3^*-2ABB_5^*+B_6^*(A^2+B^2))/4(B^2-A^2)^2\\&+(4AB^3B_5^*(B^2-A^2)+B^2B_6^*(4A^2-(A^2+B^2)^2)/4V_2\end{aligned}$$

$$L_9=-B^3B_3/8(A^2+B^2)^2+B(B_3(A^2-2B^2)-2AB_6^*)/8(B^2-A^2)^2+0.5AB^3B_6^*((B^2-A^2)/V_2-B(A^2+B^2)/V_1)$$

$$\begin{aligned}L_{10}=&\,(-A(2B^2-A^2)(2B_1^*+B_3)+(A^2+B^2)(2B_4^*+B_6^*)+BB_2^*(2B^2-A^2)-2ABB_5^*+AB_1^*(B^2-A^2))/8(B^2-A^2)\\&+(B^2(4A^2-(A^2+B^2)^2)(2B_4^*+B_6^*)+B_4^*(A^2+B^2)^2+4A^2B^3B_5^*(B^2-A^2))/8V_2\end{aligned}$$

$$\begin{aligned}L_{11}=&-(B(2B^2-A^2)(B_1^*+B_3^*)-AB_2^*(2B^2-A^2)-BB_3(B^2-A^2)-2AB(B_4^*+B_6^*)+B_5^*(A^2+B^2))/8(B^2-A^2)\\&-(4AB^3(B^2-A^2)(B_4^*+B_6^*)+B^2B_5^*(4A^2-(A^2+B^2)^2)-2ABB_6^*(A^2+B^2))/8V_2\end{aligned}$$

$$L_{12}=(BB_1^*-AB_2^*+BB_3)/8(B^2-A^2)+(2AB(A^2+B^2)(B_4^*+B_6^*)-B_5^*(A^2+B^2)^2)/8V_2$$

$$L_{13}=(-AB_1^*+BB_2^*-AB_3)/8(B^2-A^2)+(2ABB_5^*(A^2+B^2)-(A^2+B^2)$$

$$V_1=4A^2B^2(A^4+B^4)+(B^4-A^4)^2$$

$$V_2=4A^2B^2(B^4+(B^2-A^2)^2)-(B^4-A^4)^2, \quad B_1^*=B_1-B_5/8, \quad B_2^*=B_2-B_6/4, \quad B_4^*=BB_4/8, \; B_5^*=BB_5/8, \quad B_6^*=BB_6/8$$

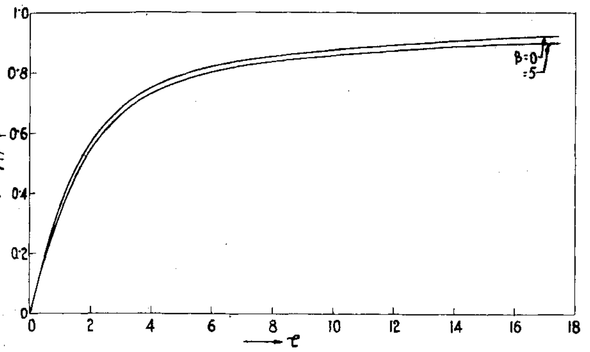

Fig. 1 Variation of surface temperature with time.

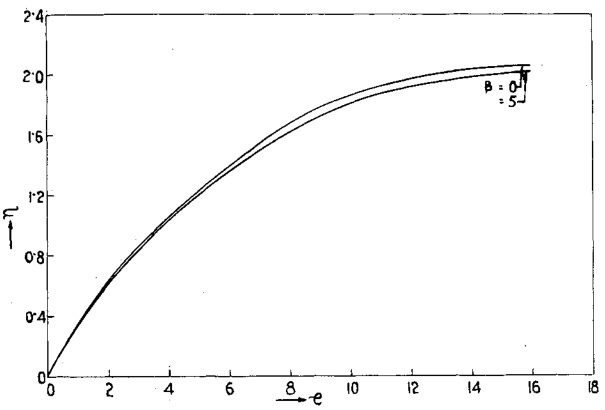

Fig. 2 Variation of melting distance with time.

For the melting solid having very high latent heat ($L\to\infty$), β is zero, and the Eq. (24) becomes

$$\dot{\phi}[3(1-\phi^4)+12\phi^3/(1-\phi^4)^3]=1 \tag{26}$$

and its solution is

$$\tau=3\phi/(1+\phi^2)+(9/8)\tan^{-1}\phi-(3/8)(1-\phi^2)^{-1}$$
$$+(9/16)\ln(1+\phi)/(1-\phi)+(3/2)(1-\phi^4)^{-2}-(9/8) \tag{27}$$

Equation (24) can also be written as

$$\tau=\int_0^1[(B_1+B_2\phi+B_3\phi^2)/(A+B\phi)(1-\phi^4)^2$$
$$+(B_4\phi^3+B_5\phi^4+B_6\phi^5)/(A+B\phi)(1-\phi_4)^3]\,d\phi \tag{28}$$

To obtain the solution, Eq. (28) is integrated numerically using Simpson's rule. The limit of integration, which varies from 0 to 1, is divided into 100 equal parts, each part being equal to 0.01. This has yielded accurate results. The surface temperature time history $\phi(\tau)$, and the melting distance time history, $\eta(\tau)$, are plotted in Figs. 1 and 2, respectively, for different values of β. It is found that for any β, both the surface temperature and melting distance increase with increase in time and that they decrease at any time with increase in β. This type of behavior also was obtained in aerodynamic ablation.[6]

Conclusion

Biot's variational method has been applied successfully in obtaining the closed-form solution for the phase-change problem with radiative heating. A study of the combined effect of radiative heating and aerodynamic heating on the ablation of melting solids is in progress.

References

[1]Lardner, T.J., "Approximate Solutions to Phase-Change Problems," *AIAA Journal*, Vol. 5, Nov. 1967, pp. 2079-2080.

[2]Biot, M.A. and Daughaday, H., "Variational Analysis of Ablation," *Journal of the Aerospace Science*, Vol. 29, Feb. 1962, pp. 227-229.

[3]Biot, M.A. and Agrawal, H.C., "Variational Analysis of Ablation for Variable Properties," *Transactions of the ASME. Sec. C, Journal of Heat Transfer*, Vol. 86, Aug. 1964, pp. 437-442.

[4]Prasad, A., "Biot's Variational Principle in a Phase-Change Problem," M.S. thesis, Oct. 1968, Dept. Mech. Eng., I.I.T. Kanpur, India.

[5]Prasad, A. and Agrawal, H.C., "Biot's Variational Principle for a Stefan Problem," *AIAA Journal*, Vol. 10, March 1972, pp. 325-327.

[6]Prasad, A. and Agrawal, H.C., "Biot's Variational Principle for Aerodynamic Ablation of Melting Solids," *AIAA Journal*, Vol. 12, Feb. 1974, pp. 250-252.

[7]Goodman, T.R., "The Heat Balance Integral and Its Application to Problems Involving a Change of Phase," *Transactions of the ASME*, Vol. 80, Feb. 1958, pp. 335-342.

Laminar Boundary-Layer Analyses for Parallel Streams with Interfacial Mass Transfer

C. K. Law*
Northwestern University, Evanston, Ill.

Introduction

RECENT studies[1-4] on transient droplet vaporization have stressed the importance of internal circulation on the vaporization characteristics through its effects on heat and mass transport rates within the droplet. This is because, although diffusional transports are always present during any transient, their rates are either much slower than, or at most comparable with, the droplet surface regression rate.[2,5] However, in the presence of internal circulation these transport rates are significantly enhanced such that, in extreme cases, even perpetual uniformity can be maintained within the droplet.[2,6] Hence an understanding of the generation and the intensity of internal circulation is an essential step toward a detailed analysis of the transient droplet vaporization problem.

An important mechanism that generates internal circulation is the shear stress induced at the nonrigid droplet surface by an external gas stream. When the relative velocity between the droplet and the gas stream is high, as is typical near the fuel spray injection port in certain power plants, it has been estimated[4] that both the liquid- and gas-phase Reynolds numbers are sufficiently large to permit the boundary-layer development on both sides of the interface. Whereas a detailed boundary-layer analysis across the interface of the droplet is obviously difficult, an estimate for the amount of induced liquid-phase motion can be obtained by approximating the shoulder region of the droplet as a flat surface.

Lock[7] analyzed the boundary-layer velocity distribution between two parallel streams, with dissimilar freestream velocities and fluid properties, in the absence of interfacial

Received Jan. 14, 1976; revision received June 16, 1976. This work has been sponsored by the National Science Foundation Grant NSF-RANN AER75-09538.

Index categories: Boundary Layers and Convective Heat Transfer – Laminar; Multiphase Flows; Combustion in Heterogeneous Media.

*Associate Professor, Department of Mechanical Engineering and Astronautical Sciences. Member AIAA.